Inorganic Chemistry

Article

pubs.acs.org/IC

Calorimetric Assessment of Fe^{2+} Binding to α-Ketoglutarate/Taurine Dioxygenase: Ironing Out the Energetics of Metal Coordination by the 2-His-1-Carboxylate Facial Triad

Kate L. Henderson,[†] Tina A. Müller,[‡] Robert P. Hausinger,[‡] and Joseph P. Emerson*[,†]

[†]Department of Chemistry, Mississippi State University, Mississippi State, Mississippi 39762, United States

[‡]Department of Microbiology and Molecular Genetics, Michigan State University, East Lansing, Michigan 48824-4320, United States

Supporting Information

ABSTRACT: The thermodynamic properties of Fe^{2+} binding to the 2-His-1-carboxylate facial triad in α-ketoglutarate/taurine dioxygenase (TauD) were explored using isothermal titration calorimetry. Direct titrations of Fe^{2+} into TauD and chelation experiments involving the titration of ethylenediaminetetraacetic acid into Fe^{2+}-TauD were performed under an anaerobic environment to yield a binding equilibrium of 2.4 ($\pm$0.1) $\times$ 10^7 (K_d = 43 nM) and a ΔG° value of $-$10.1 ($\pm$0.03) kcal/mol. Further analysis of the enthalpy/entropy contributions indicates a highly enthalpic binding event, where ΔH = $-$11.6 ($\pm$0.3) kcal/mol. Investigations into the unfavorable entropy term led to the observation of water molecules becoming organized within the Fe^{2+}-TauD structure.

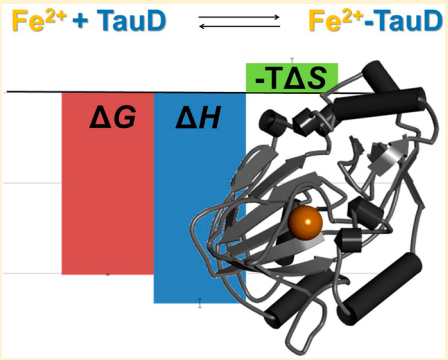

INTRODUCTION

Mononuclear Fe^{2+} sites can be found throughout nature at the catalytic centers of many important enzymes.[1−3] Many complexes of Fe^{2+} spontaneously react with dioxygen to generate high-valent intermediates that are fundamental for the biological and environmental processes they catalyze. A common motif found in a range of nonheme Fe^{2+} oxygenases is the 2-His-1-carboxylate facial triad.[4,5] This metal-binding configuration involves the side chains of two histidine and one aspartate/glutamate amino acid residues to occupy one face of the Fe^{2+} octahedral coordination sphere, leaving the adjacent face coordinated to solvent ligands, which are easily exchanged for binding substrates (Figure 1A). In the dioxygenase family of enzymes, the 2-His-1-carboxylate facial triad affords proximity of the substrate(s) and dioxygen to ensure efficient catalysis of reactions such as the repair of alkylated DNA/RNA, the biosynthesis of penicillin, and the degradation of aromatic compounds for carbon sequestration.[6−9]

A subfamily of oxygenases containing the 2-His-1-carboxylate motif are the α-ketoglutarate (αKG)-dependent enzymes.[10] The best studied member of this subfamily is αKG/taurine dioxygenase or taurine hydroxylase (TauD), an enzyme that couples the oxidative decarboxylation of αKG and oxidation of taurine to liberate sulfite (Scheme 1).[11] In TauD, the mononuclear Fe^{2+} center is coordinated facially to the side chains of residues His99, Asp101, and His255 (Figure 1B). This affords the bidentate binding of αKG on the adjacent face, with the carbonyl oxygen binding trans to the Asp ligand and the C1 carboxylate oxygen binding across from His99.[12,13] The final coordination site is open for dioxygen binding and activation. Previous studies have indicated that several divalent metals can

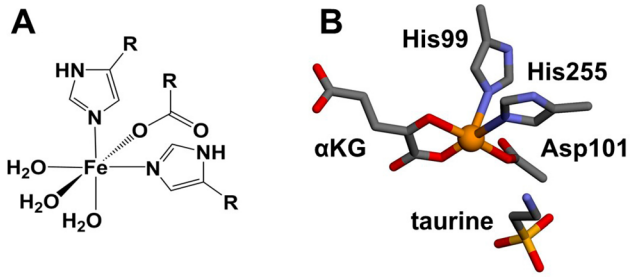

Figure 1. (A) Representation of the 2-His-1-carboxylate facial triad, where the histidine and carboxylate side chains are bound to one face of the iron. The adjacent sites of the coordination sphere are solvated until the cofactor and substrates bind. (B) Structure of the Fe^{2+}-TauD active site pocket, with His99, Asp101, and His255 making up the 2-His-1-carboxylate facial triad. αKG chelates with Fe^{2+} (orange sphere), and taurine is bound nearby but does not coordinate with Fe^{2+}. The coordinates were taken from PDB:1OS7.[12]

Scheme 1. Reaction Catalyzed by TauD

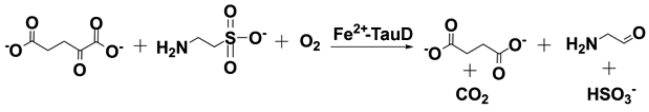

Received: December 2, 2014
Published: February 10, 2015

DOI: 10.1021/ic502881q
Inorg. Chem. 2015, 54, 2278−2283

bind to the active site of TauD; however, Fe^{2+} is the only metal that is capable of supporting its catalytic activity.[14,15] On the basis of perturbations to the protein UV absorbance spectrum, K_d of Fe^{2+} binding to TauD apoprotein was reported to be 90 ± 50 nM.[14] Here, we explore the thermodynamic properties of Fe^{2+} binding to TauD and discuss the underlying driving forces behind Fe^{2+} coordination by the 2-His-1-carboxylate facial triad.

MATERIALS AND METHODS

Reagents and General Procedures. All reagents and buffers were of the highest grade available and were used as received. All solutions and media were prepared in 18 MΩ water purified through a Millipore system. Glass dialysis containers and vials for apoprotein storage were rinsed with ethylenediaminetetraacetic acid (EDTA) and thoroughly rinsed with 18 MΩ water before use.

Overexpression and Purification of α-Ketoglutarate (αKG)/Taurine Dioxygenase (TauD). TauD was produced in *Escherichia coli* BL21(DE3) cells harboring plasmid pME4141.[15] Cultures were grown at 30 °C and induced by the addition of 0.1 mM isopropyl-β-D-1-thiogalactose. Cells were harvested by centrifugation and resuspended in TE (25 mM Tris buffer, pH 8.0, and 1 mM EDTA) containing 1 mM phenylmethylsulfonyl fluoride. Cell-free extracts were prepared by sonication followed by centrifugation at 100000*g* for 1 h. The lysate (approximately 50 mL) was applied to a (diethylamino)ethyl−Sepharose column (2.5 × 19 cm, Sigma) equilibrated with TE, and protein was eluted using a three-step protocol: a linear gradient of 0−0.25 M NaCl in TE for 2 column volumes (CVs), isocratic flow of 0.25 M NaCl in TE (1 CV), followed by a linear gradient from 0.25 to 1 M NaCl in TE in 1 CV. Fractions were analyzed by sodium dodecyl sulfate polyacrylamide gel electrophoresis, and those containing TauD were pooled, concentrated using a centrifugal filter (Millipore), and dialyzed overnight into TE containing 0.5 M $(NH_4)_2SO_4$. The sample was loaded onto a phenyl−Sepharose column (2.6 × 20 cm, GE Healthcare) equilibrated with a TE buffer containing 0.5 M $(NH_4)_2SO_4$. TauD was eluted using a gradient from 0.5 to 0.05 M $(NH_4)_2SO_4$ in TE (1 CV) followed by decreasing $(NH_4)_2SO_4$ concentration to 0 M in TE for 0.75 CV. Fractions were analyzed and concentrated as before and dialyzed into TE. When appropriate, TauD was further purified by gel filtration chromatography using Superdex-200 with a TE buffer containing 150 mM NaCl. Eluted TauD was again concentrated and dialyzed into TE. Purified TauD was stored in aliquots at −80 °C.

Enzyme activity assays were carried out by incubating TauD (3−5 μg/mL) in an assay buffer containing 25 mM Tris, pH 8, 1 mM taurine, 1 mM αKG, 50 μM Fe^{2+}, and 100 μM ascorbate for 1−5 min at 37 °C. The assays were stopped by the addition of EDTA (5 mM), and sulfite production was determined spectrophotometrically at 415 nm after the addition of Ellman's reagent (0.1 mg/mL final concentration). One unit of enzyme activity is defined as the amount of enzyme that releases 1 μmol of sulfite/min at 37 °C.

Isothermal Titration Calorimetry (ITC). Purified TauD apoprotein stock was diluted to 100 μM and dialyzed against one of three different 25 mM buffers (as specified) at pH 7.4 for 18 h. TauD and dialysate were made anaerobic by passing argon over the solutions. A 3.3 mM iron(II) acetate solution was made by using the degassed dialysate. The MicroCal VP-ITC instrumentation was sealed in an anaerobic chamber (Plaslabs) with a constant dinitrogen flow during the course of the experiment. Data were collected at 25 °C, unless specified otherwise, for 3 μL injections of the iron(II) acetate solution into a 1.5 mL cell containing the TauD solution to generate Fe^{2+}-TauD. Injections were carried out at a stirring rate of 307 rpm over 6 s periods with 300 s spacings between injections. Chelation titration experiments were performed with 50 μM anaerobic Fe^{2+}-TauD and 800 μM EDTA in a 25 mM HEPES buffer at pH 7.4. Data were collected at 25 °C for 6 μL injections of EDTA over 12 s periods with 300 s spacings between injections at a stirring rate of 307 rpm. For all experimental sets, control experiments were performed and raw heats were subtracted as necessary. The integrated heats obtained by titrating buffer into buffer or Fe^{2+} into buffer (Figure S1 in the Supporting Information, SI) were negligible. Data were analyzed using a one-site model in the *MicroCal* data analysis software package in *Origin* (OriginLabs) and using *CHASM* software, developed by the laboratory of Edwin Lewis (Mississippi State University), which uses a nonlinear least-squares fitting algorithm to fit the change in heat per injection to equilibrium binding model equations.[16] The isotherms for Fe^{2+} binding to TauD in various buffers were replicated 2−4 times.

RESULTS

Binding of metal ions by macromolecules can be monitored by ITC through the direct measurement of the heat changes associated with the binding reaction.[17,18] In a single experiment, the binding equilibrium (K) and observed enthalpy (ΔH_{obs}) can be directly obtained, permitting calculation of the Gibbs free energy ($\Delta G°$) and entropy (ΔS) terms using eqs 1 and 2.

$$\Delta G° = -RT \ln K \tag{1}$$

$$\Delta G° = \Delta H_{obs} - T\Delta S \tag{2}$$

All entropy terms in this study are reported in terms of $-T\Delta S$ in order to provide a straightforward comparison to the ΔG and ΔH terms.

The observed enthalpy terms obtained from metal binding ITC experiments are more appropriately described as a complex series of competitive binding events that involve the Fe^{2+} ion. Moreover, these competitive binding events often result in the release or uptake of protons, resulting in ionization of the buffer ($\Delta H_{ionization}$). A plot of ΔH_{obs} versus $\Delta H_{ionization}$ yields a linear relationship, where the slope is equal to the number of protons (n_p) released/consumed during the binding event, as shown in eq 3.

$$\Delta H_{obs} + \Delta H_{Fe\text{-}buffer} = (\Delta H_{Fe\text{-}TauD} - n_p \Delta H_{Fe\text{-}TauD\text{-}H}) + n_p(\Delta H_{ionization}) \tag{3}$$

Control experiments involving the titration of Fe^{2+}-buffer complexes into EDTA were performed to elucidate $\Delta H_{Fe\text{-}buffer}$ for our thermodynamic analyses (see Figures S2−S4 and the corresponding thermodynamic cycles in Tables S1−S3 in the SI). These experiments were performed in 2-(carbamoylmethylamino)ethanesulfonic acid (ACES), 2-(*N*-morpholino)ethanesulfonic acid (MOPS), and 2-[4-(2-hydroxyethyl)piperazin-1-yl]ethanesulfonic acid (HEPES) buffers, which were chosen for their pH range and minimal heats of interaction with the metal ion or protein. For the direct titration of iron(II) acetate into a solution of TauD apoprotein, the raw data were baseline-corrected and the isotherms were fit for binding at a single site, yielding ΔH_{obs} values in ACES, MOPS, and HEPES buffers (Figure 2). A plot of ΔH_{obs} + $\Delta H_{Fe\text{-}buffer}$ against $\Delta H_{ionization}$ indicates that 0.9 protons are released during the binding event, and the y intercept of −1.40 kcal/mol is the heat associated with Fe^{2+} binding to TauD minus the protonation enthalpy of TauD ($\Delta H_{Fe\text{-}TauD\text{-}H}$), as illustrated in Figure 2C. A complete list of the observed thermodynamic parameters for the direct titration of Fe^{2+} into TauD in each buffer can be found in Table 1. Error bars on the data points obtained in an ACES buffer are larger in magnitude than those observed for other buffers because of the averaging of titrations between different preparations of TauD. However, because of the goodness of fit in our slope (R^2 = 1.00), we believe the data to be accurate and represent the average thermodynamic values for Fe^{2+} binding to TauD.

DOI: 10.1021/ic502881q
Inorg. Chem. 2015, 54, 2278−2283

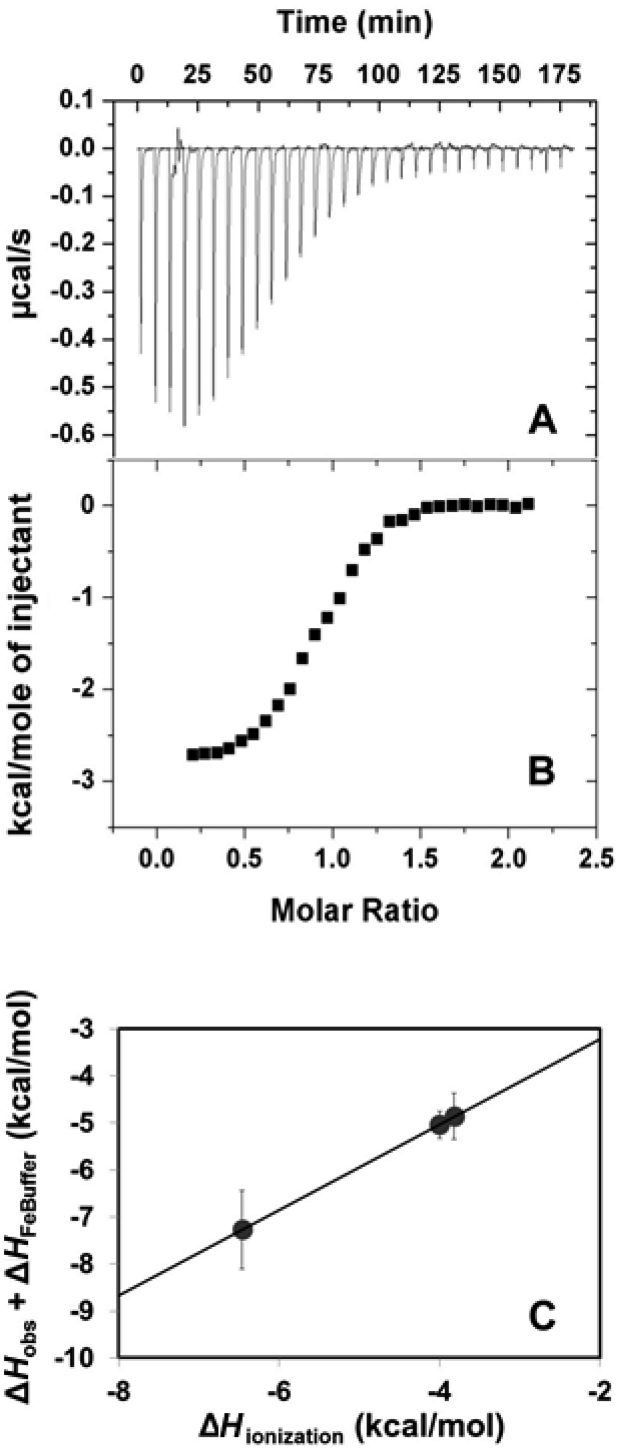

Figure 2. Representative raw heat (A) and integrated isotherm (B) for Fe^{2+} binding to TauD in a MOPS buffer. Observed enthalpies versus ionization enthalpies of the ACES, MOPS, and HEPES buffers (C). The slope of the line yields the number of protons released from the system. The linear fit is $y = 0.91x - 1.40$. $R^2 = 1.00$.

Using the observed enthalpy values from the titrations of Fe^{2+} into TauD, thermodynamic cycles can be generated that incorporate all known equilibria taking place in a solution for the Fe^{2+} titration in each buffering system (Table 2 for MOPS buffer and Tables S5 and S6 in the SI for ACES and HEPES buffers, respectively). Cycles similar to these have been used in analysis of the metal binding to small peptides and protein systems.[19−21] The overall reaction contains dissociation of the Fe^{2+} ion from the Fe^{2+}-buffer complex, Fe^{2+} binding to the 2-His-1-carboxylate facial triad, and protonation of the buffer, which stems from a loss of 0.9 protons, presumably from the Fe^{2+} bound water molecules due to a shift in the pK_a when bound to the metal. Deconvolution of the observed enthalpy data in MOPS results in an estimation of $\Delta H_{\text{Fe-TauD}}$ as −11.5 (±0.2) kcal/mol. A complete list of the changes in the enthalpy for Fe^{2+} binding to TauD from the thermodynamic cycles in each buffer can be found in Table 3.

The additional equilibria in solution also have an effect on the observed K value in the direct titration of Fe^{2+} into TauD. Because there are interactions between metal ions and buffers, K for the direct titration is the product of the individual equilibrium constants occurring in solution. This includes the association constant (K_a) of Fe^{2+}-TauD and the dissociation constant ($K_{\text{d,Fe-buffer}}$) of the Fe^{2+} buffer. To obtain the K_a term of Fe^{2+}-TauD, a second set of experiments was performed involving a chelation titration where the Fe^{2+}-EDTA binding equilibrium ($K_{\text{Fe-EDTA}}$) is known, allowing for calculation of the Fe^{2+}-TauD K_a using the following equation:[20]

$$K_a = K_{\text{Fe-EDTA}}/K \quad \text{where } K_a = 1/K_{\text{d,Fe-TauD}} \tag{4}$$

The integrated isotherm from the ITC chelation titration of EDTA into Fe^{2+}-TauD in a 25 mM HEPES buffer at pH 7.4 is shown in Figure 3 (shown in blue). The integrated isotherm of the observed chelation includes one-site binding with a significant endothermic feature associated with the dilution of EDTA into a buffer solution. These dilutions appear to be associated with a second binding process, seen in both direct titration and chelation experiments for TauD and other enzyme systems. This second process could be attributed to a weak, adventitious binding site[13] or structural rearrangements of the new Fe^{2+}-EDTA complex. A nonprotein Fe^{2+} ITC control experiment was performed, and the data (Figure 3, shown in red) are subtracted to yield a more symmetric one-site binding event (Figure 3, gray).[20] The K value for the chelation titration is 8.4 (±0.4) × 10^6. As shown in Scheme 2, deconvolution of the series of equilibria taking place in the chelation experiment yields a K_a value for Fe^{2+}-TauD of 2.4 (±0.1) × 10^7 [or a K_d value of 42 (±2) nM, in excellent agreement with the previously published value].[14] This K_a value then allows for the back-calculation of $K_{\text{a,Fe-buffer}}$ from the set of direct titration experiments, which is found in Table 1. Using the association constant for Fe^{2+} binding to TauD ($K_{\text{Fe-TauD}}$) and $\Delta H_{\text{Fe-TauD}}$, we obtain a $\Delta G°$ value of −10.1 (±0.03) kcal/mol and a $-T\Delta S$ contribution of −12.1 (±0.03) kcal/mol, indicating an enthalpy-driven binding event. A complete thermodynamic profile is illustrated in Figure 4.

A heat capacity study was performed to help determine the nature of the unfavorable entropy term during the Fe^{2+} coordination event. By the Fe^{2+} binding titration was performed at different temperatures and the observed enthalpy was plotted against temperature, the change in the heat capacity (ΔC_p) was determined by the slope of the linear correlation between points.[22−25] The direct titration of Fe^{2+} into TauD in a MOPS buffer was performed at 5, 15, and 25 °C. The plot of ΔH_{obs} versus temperature yields a ΔC_p value of 0.0389 (±0.0138) kcal/mol·K (Figure 5). Using the statistical thermodynamics equation of $\Delta C_p = N3R$, where R is the gas constant and N is the number of solvent molecules gained/released, the Fe^{2+} binding to TauD event has a net gain of approximately 6.5 (±2.3) water molecules.

DOI: 10.1021/ic502881q
Inorg. Chem. 2015, 54, 2278−2283

Table 1. Observed Thermodynamic Values from the ITC Titration of Iron(II) Acetate into TauD[a]

25 mM buffer (pH 7.4)	n	K	ΔH_{obs} (kcal/mol)	$\Delta H_{ionization}$ (kcal/mol)	ΔG (kcal/mol)	$-T\Delta S_{obs}$ (kcal/mol)	$K_{Fe\text{-}buffer}$
MOPS	0.78 (±0.13)	5.4 (±0.7) × 10^5	−2.2 (±0.3)	−5.04	−7.8 (±0.1)	−5.7 (±0.4)	42.0 (±5)
HEPES	0.85 (±0.13)	3.3 (±0.6) × 10^5	−1.9 (±0.5)	−4.86	−7.5 (±0.1)	−5.6 (±0.4)	72.5 (±14)
ACES	0.94 (±0.07)	1.0 (±0.7) × 10^7	−3.9 (±0.8)	−7.27	−9.2 (±1.0)	−5.3(±1.5)	19.7 (±13)

[a]Values are the average of 2−4 replicates, and the errors associated with the values are 1 standard deviation from the mean.

Table 2. Thermodynamic Cycle for Fe^{2+} Binding to TauD in a MOPS Buffer

reaction	coefficient	ΔH (kcal/mol)
Fe^{2+}-MOPS + TauD-$H^+_{0.9}$ ⇄ Fe^{2+}-TauD + MOPS-$H^+_{0.9}$ + 0.1 MOPS		−2.17[a]
Fe^{2+}-MOPS ⇄ Fe^{2+} + MOPS	1.0	1.83[b]
Fe^{2+}-TauD-H ⇄ Fe^{2+}-TauD + H^+	0.91	13.34[c]
MOPS + H^+ ⇄ MOPS-H^+	0.91	−5.04[d]
Fe^{2+} + TauD ⇄ Fe^{2+}-TauD	1.0	−11.55

[a]From Table 1. [b]Calculated from the control experiments of EDTA chelation of Fe^{2+} in a MOPS buffer. [c]Represents the ionization of water within the H_2O−Fe^{2+}-TauD complex deprotonating to the HO−Fe^{2+}-TauD species. Value is taken from ref 26. [d]Value taken from ref 30.

Table 3. Average Enthalpy Values in Each Buffer for Fe^{2+} Binding to TauD

25 mM buffer, pH 7.4	$\Delta H_{Fe\text{-}TauD}$ (kcal/mol)	25 mM buffer, pH 7.4	$\Delta H_{Fe\text{-}TauD}$ (kcal/mol)
MOPS	−11.46 (±0.01)	ACES	−11.94 (±0.83)
HEPES	−11.53 (±0.49)	average	−11.64 (±0.25)

Values were calculated based on the thermodynamic cycle for the binding reaction in the respective buffering system. Values were averaged, and the error represents 1 standard deviation from the mean.

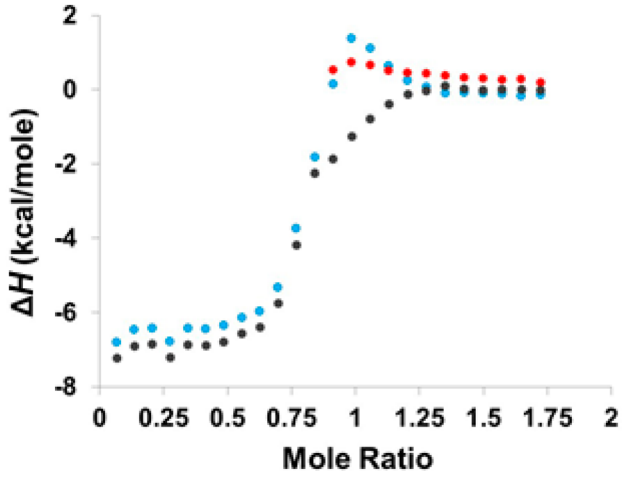

Figure 3. Titration of EDTA into Fe^{2+}-TauD. Integrated data (blue), nonprotein Fe^{2+} control (red), and the baseline subtracted, adjusted isotherm (gray).

DISCUSSION

Nature has adapted to provide a few common metal-binding sites to catalyze oxidation reactions in biology. The 2-His-1-carboxylate facial triad motif is often detected in nonheme oxygenase enzymes, where the representative carboxylate ligand is either a glutamate or aspartate residue.[1] This residue supplies a negative charge in the binding motif, dramatically stabilizing

Scheme 2. Thermodynamic Cycle for Fe^{2+} Binding to TauD

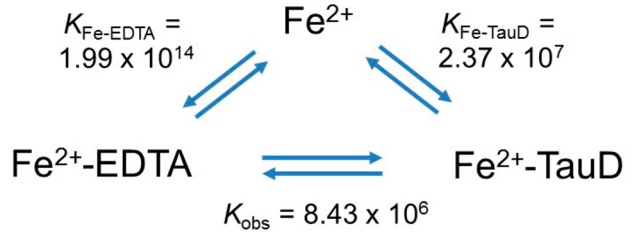

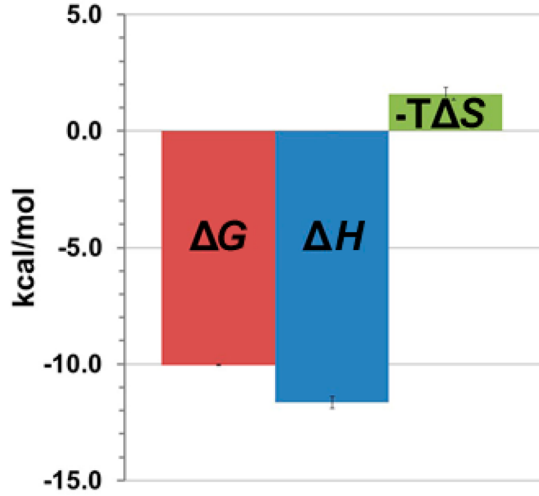

Figure 4. Complete thermodynamic profile for Fe^{2+} binding to TauD. Fe^{2+}-buffer interactions and buffer ionization have been accounted for to give a more accurate representation of the thermodynamic properties for the Fe^{2+} binding event.

the divalent metal ion and lowering the overall charge on the Fe^{2+} complex. In this study, we measured Fe^{2+} binding to TauD as a means of directly determining the thermodynamic driving forces behind the 2-His-1-carboxylate facial triad coordination of the metal ion in a representative of this family of nonheme Fe^{2+} oxygenases.

Fe^{2+} binding to the 2-His-1-carboxylate facial triad in TauD is a highly favorable reaction in which one metal ion binds per monomer with a $\Delta G°$ value of −10.1 (±0.03) kcal/mol. The substoichiometric number of metal ions (n) bound to TauD (Table 1) may be due to residual divalent metal ions contaminating the metal ion in the solution of the apoprotein. A control experiment was performed where EDTA was titrated into apoprotein (see Figure S5 in the SI), resulting in approximately 0.2 mol equiv of Fe^{2+} (or other cation) binding to EDTA. This result justifies the substoichiometric metal content for the direct titration experiments.

The favorable $\Delta G°$ of Fe^{2+} binding to TauD is driven by the enthalpic contribution of the coordination process. Included in the observed enthalpy term (approximately −2.8 kcal/mol) is the Fe^{2+} coordination to His99, Asp101, and His255, as well as a proton release event. We hypothesize that this proton release

DOI: 10.1021/ic502881q
Inorg. Chem. 2015, 54, 2278−2283

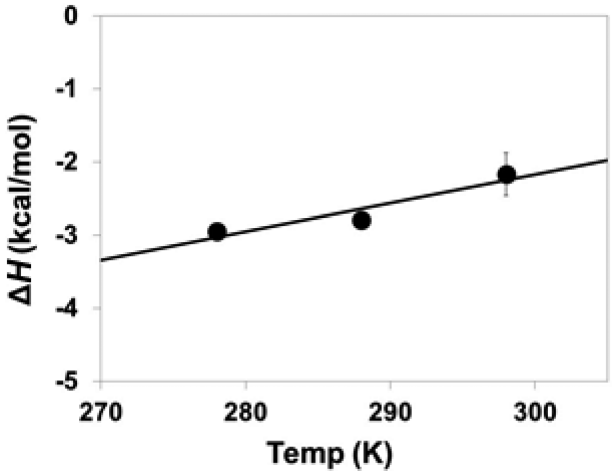

Figure 5. Effect of the temperature on ΔH of Fe^{2+} binding to TauD. The calculated ΔH associated with Fe^{2+} titration into TauD at various temperatures in a MOPS buffer at pH 7.4 yields a slope equal to that of ΔC_p for the binding reaction. Values are averaged. and the error is 1 standard deviation from the mean. The data (Table S4) are found in the SI.

event is associated with ionization of water coordinated to the Fe^{2+} ion. The Lewis acidity of the metal ion results in an average reduction in the pK_a value of the coordinated water molecules to approximately 7.8; however, each coordinated water molecule most likely has a unique pK_a value that is slightly shifted based on its exact location in the coordination sphere and its hydrogen-bonding network. The net release of 0.9 protons as a result of this event provides an additional 12.0 kcal/mol in enthalpic instability for Fe^{2+} binding. When the proton release and buffer ionization are accounted for, the change in enthalpy (ΔH) for Fe^{2+} binding is a highly favorable −11.6 (±0.3) kcal/mol. Alternatively, some proton density could be released from His255 and His99 when Fe^{2+} binds. At pH 7.4, approximately 96% of free histidine in solution is in neutral form. If the histidines within the active site pocket are in this protonation state, then the Lewis acidity of the Fe^{2+} ion when bound to the ε nitrogen will lower the pK_a value of the proton residing on the δ nitrogen, which could result in additional proton loss. The ionization enthalpy of the δ nitrogen for a free histidine residue has been reported to be 10.5 kcal/mol,[26,27] which would also have a destabilizing effect on the enthalpy of Fe^{2+} binding to TauD, much like water as proposed above and within approximately 3 kcal/mol of the enthalpy value. However, the ionization enthalpy values of histidine bound to Fe^{2+} are not known, hindering accurate thermodynamic analysis for this possibility.

There are few comparable Fe^{2+} binding studies in the literature. One recent report measured Fe^{2+} binding to the histidine-rich peptide sequence of the iron-regulated transporter IRT1, yielding a ΔH value of −6.5 kcal/mol; however, it is unclear whether or not this value includes the ionization of water.[19] The difference in the enthalpy between this system and TauD could lie in the contribution of the aspartate side-chain residue, where the negatively charged residue provides charge stabilization with the positively charged Fe^{2+}, which, in turn, would have direct effects on the enthalpy and entropy terms for the system. In another example, Fe^{2+} binding to an α-helical-rich keratin complex suggests Fe^{2+} coordination to two glutamate residues within the α-helix, which supplies an observed enthalpy of −0.86 kcal/mol.[28] This enthalpic value is largely due to complete charge stabilization between the two negatively charged glutamate side-chain residues and the divalent metal ion (accounting for a large binding equilibrium of 2.8×10^5), whereas a negligible enthalpy indicates a highly entropically driven binding event, as expected by charge−charge interactions.[29] Our results indicate a large binding equilibrium and a distinctly favorable change in the enthalpy for Fe^{2+} binding to TauD. This result is consistent with charge stabilization contributions from the aspartate residue in addition to the favorable contacts with the histidine side-chain residues to provide favorable thermodynamic terms. However, solvation and conformational changes also play a role in the free energy of metal-ion coordination, limiting a detailed comparison of TauD with IRT1 and keratin.

The entropy term for Fe^{2+} binding to TauD is slightly unfavorable, indicated by a $-T\Delta S$ term of +1.6 (±0.4) kcal/mol. The unfavorable entropy compensation for enthalpically driven reactions in macromolecular systems usually stems from structural reorganization upon the binding event. However, previous structural and spectroscopic studies on Fe^{2+} binding to TauD indicate that there is no substantial structural reorganization when the enzyme coordinates Fe^{2+}.[12−14] Likely candidates accounting for the small, unfavorable $-T\Delta S$ value include an altered hydrogen-bonding network between amino acid residues once Fe^{2+} is bound, an overall gentle relaxation of the TauD structure providing more flexibility to the enzyme, water reorganization within or at the surface of the enzyme, proton release, as indicated by our ITC titration studies, and buffer release (approximately 1−2 molecules per metal ion, dependent on the buffer used) to bulk solvent from the Fe^{2+}-buffer complex. The orchestration of all of these terms during the dynamic Fe^{2+} binding reaction, in addition to charge stabilization at the Fe^{2+} center, may result in a negligible net change during metal coordination; this would explain why the entropy term is so small. To gain insight into the role of solvent in the metal coordination process, we have also performed metal titrations at a series of temperatures, which gives rise to the heat capacity of Fe^{2+} binding to TauD. Although there are no major structural changes associated with the metal-ion coordination to TauD, this study indicates a small, positive change in the heat capacity (+38.9 cal/mol·K) over a 20 °C temperature range. As the temperature increases, our observed data reflect a decrease in ΔH, while a slight increase in $-T\Delta S$ occurs. Higher temperatures can cause more favorable ΔS terms, where overall increases in the vibrational and rotational energies are more pronounced, which could contribute to the more favorable $-T\Delta S$ term. This process creates balance between the enthalpy and entropy terms, resulting in no net change in ΔG_{obs} over the 20 °C temperature range.

When we further analyze the ΔC_p term using statistical thermodynamics, the positive ΔC_p value corresponds to the ordering of approximately 6.5 water molecules within Fe^{2+}-TauD upon metal coordination to the 2-His-1-carboxylate ligands. This result can be rationalized as a shift in the hydrogen-bonding network surrounding the metal binding site, where local water molecules help to stabilize the organized structure once Fe^{2+} is bound. This notion also helps to explain the source of unfavorable entropy measured from this equilibrium.

■ CONCLUSION

The data presented herein combine the direct titration of nonheme Fe^{2+} into TauD with the chelation titration of EDTA

DOI: 10.1021/ic502881q
Inorg. Chem. 2015, 54, 2278−2283

into Fe^{2+}-TauD to obtain all of the thermodynamic properties for nonheme Fe^{2+} coordination to the 2-His-1-carboxylate facial triad of TauD (Scheme 2). The complete binding process yields a highly favorable ΔG° value of −10.1 (±0.03) kcal/mol and is clearly an enthalpy-driven process that releases 0.9 protons from bound water molecules coordinated to the metal center. Upon Fe^{2+} binding, water is reorganized within the Fe^{2+}-TauD structure, suggesting a change in the hydrogen-bonding network within the enzyme. This provides clarity to the driving forces behind Fe^{2+} binding in TauD. However, it remains to be seen if this trend is generalized across the 2-His-1-carboxylate facial triad enzymes.

■ ASSOCIATED CONTENT

Ⓢ Supporting Information

ITC experiments and thermodynamic data. This material is available free of charge via the Internet at http://pubs.acs.org.

■ AUTHOR INFORMATION

Corresponding Author

*E-mail: jemerson@chemistry.msstate.edu. Phone: 662-325-9500. Fax: 662-325-1618.

Notes

The authors declare no competing financial interest.

■ ACKNOWLEDGMENTS

We thank Salette Martinez for assistance with one preparation of enzyme. This work was supported by the National Institutes of Health (Grant GM063584 to R.P.H.) and start-up funds through Mississippi State University (to J.P.E.).

■ REFERENCES

(1) Que, L., Jr.; Ho, R. Y. N. *Chem. Rev.* **1996**, *96*, 2607−2624.
(2) Leitgeb, S.; Nidetzky, B. *Biochem. Soc. Trans.* **2008**, *36*, 1180−1186.
(3) Costas, M.; Mehn, M. P.; Jensen, M. P.; Que, L., Jr. *Chem. Rev.* **2004**, *104*, 939−986.
(4) Hegg, E. L.; Que, L., Jr. *Eur. J. Biochem.* **1997**, *250*, 625−629.
(5) Koehntop, K. D.; Emerson, J. P.; Que, L., Jr. *J. Biol. Inorg. Chem.* **2005**, *10*, 87−93.
(6) Yi, C.; Jia, G.; Hou, G.; Dai, Q.; Zhang, W.; Zheng, G.; Jian, X.; Yang, C. G.; Cui, Q.; He, C. *Nature* **2010**, *468*, 330−333.
(7) Zheng, G.; Dahl, J. A.; Niu, Y.; Fedorcsak, P.; Huang, C. M.; Li, C. J.; Vagbo, C. B.; Shi, Y.; Wang, W. L.; Song, S. H.; Lu, Z.; Bosmans, R. P.; Dai, Q.; Hao, Y. J.; Yang, X.; Zhao, W. M.; Tong, W. M.; Wang, X. J.; Bogdan, F.; Furu, K.; Fu, Y.; Jia, G.; Zhao, X.; Liu, J.; Krokan, H. E.; Klungland, A.; Yang, Y. G.; He, C. *Mol. Cell* **2013**, *49*, 18−29.
(8) Kovaleva, E. G.; Lipscomb, J. D. *Nat. Chem. Biol.* **2008**, *4*, 186−193.
(9) Baldwin, J. E.; Bradley, M. *Chem. Rev.* **1990**, *90*, 1079−1088.
(10) Hausinger, R. P. *Crit. Rev. Biochem. Mol. Biol.* **2004**, *39*, 21−68.
(11) Proshlyakov, D. A., Hausinger, R. P. *Iron-Containing Enzymes Versatile Catalysts of Hydroxylation Reactions in Nature*; de Visser, S. P., Kumar, D., Eds.; Royal Society of Chemistry: London, 2012; pp 67−87.
(12) O'Brien, J. R.; Schuller, D. J.; Yang, V. S.; Dillard, B. D.; Lanzilotta, W. N. *Biochemistry* **2003**, *42*, 5547−5554.
(13) Elkins, J. M.; Ryle, M. J.; Clifton, I. J.; Dunning Hotopp, J. C.; Lloyd, J. S.; Burzlaff, N. I.; Baldwin, J. E.; Hausinger, R. P.; Roach, P. L. *Biochemistry* **2002**, *41*, 5185−5192.
(14) Grzyska, P. K.; Hausinger, R. P.; Proshlyakov, D. A. *Anal. Biochem.* **2010**, *399*, 64−71.
(15) Eichhorn, E.; van der Ploeg, J. R.; Kertesz, M. A.; Leisinger, T. *J. Biol. Chem.* **1997**, *272*, 23031−23036.
(16) Le, V.; Buscaglia, R.; Chaires, J. B.; Lewis, E. A. *Anal. Biochem.* **2012**, *434*, 233−241.
(17) Wilcox, D. E. *Inorg. Chim. Acta* **2008**, *361*, 857−867.
(18) Grossoehme, N. E.; Spuches, A. M.; Wilcox, D. E. *J. Biol. Inorg. Chem.* **2010**, *15*, 1183−91.
(19) Grossoehme, N. E.; Akilesh, S.; Guerinot, M. L.; Wilcox, D. E. *Inorg. Chem.* **2006**, *45*, 8500−8508.
(20) Song, H.; Wilson, D. L.; Farquhar, E. R.; Lewis, E. A.; Emerson, J. P. *Inorg. Chem.* **2012**, *51*, 11098−11105.
(21) Grossoehme, N. E.; Mulrooney, S. B.; Hausinger, R. P.; Wilcox, D. E. *Biochemistry* **2007**, *46*, 10506−10516.
(22) Sturtevant, J. M. *Proc. Natl. Acad. Sci. U.S.A.* **1977**, *74*, 2236−2241.
(23) Cooper, A.; Johnson, C. M.; Lakey, J. H.; Nollmann, M. *Biophys. Chem.* **2001**, *93*, 215−230.
(24) Cooper, A. *Biophys. Chem.* **2000**, *85*, 25−39.
(25) Cooper, A. *Biophys. Chem.* **2005**, *115*, 89−97.
(26) *NIST Standard Reference Database 46*, version 7.0; NIST: Gaithersburg, MD, 2003.
(27) Zhang, Y.; Akilesh, S.; Wilcox, D. E. *Inorg. Chem.* **2000**, *39*, 3057−3064.
(28) Zhao, Y.; Marzinek, J. K.; Bond, P. J.; Chen, L.; Li, Q.; Mantalaris, A.; Pistikopoulos, E. N.; Noro, M. G.; Han, L.; Lian, G. *J. Pharm. Sci.* **2014**, *103*, 1224−32.
(29) Gitlin, I.; Carbeck, J. D.; Whitesides, G. M. *Angew. Chem., Int. Ed.* **2006**, *45*, 3022−3060.
(30) Goldberg, R. N.; Kishore, N.; Lennon, R. M. *J. Phys. Chem. Ref. Data* **2002**, *31*, 231−370.

DOI: 10.1021/ic502881q
Inorg. Chem. 2015, 54, 2278−2283